Study of Stress Induced Problem in Headrace Tunnel of Nilgirikhola Hydroelectric Project

Chet Nath Neupane [a], Trilok Chandra Bhatta [b], Biplove Ghimire [c]

a, b, c *Department of Civil Engineering, Pashchimanchal Campus, IOE, Tribhuvan University, Nepal*
b *Visiting Faculty*
✉   a dipenneupane666@gmail.com, b bhattatrilok.vucl@gmail.com, c biplovegmeray@gmail.com

Abstract
As a result of tectonic action, the rock masses of Nepal Himalaya are severely folded, faulted, sheared, fractured and deeply worn. It has been difficult to effectively predict rock mass quality and analyze stress-induced difficulties in the Nepal Himalayas, where tunnel squeezing is common in weak rock and weakness zones. Tunnel squeezing can occur in incompetent rock, which is highly weak, schistose, and malleable, because a plastic zone arises around the tunnel, causing excessive deformation in the tunnel periphery. Tangential stress in competent and brittle rock with high levels of stress due to excessive overburden exceeds the strength of the rock mass, resulting in rock spalling or rock burst difficulties. This paper focuses on stress-induced problems in tunnel construction that impact project performance. It involves a literature review using geological data, case studies, and field data to assess and predict issues. Rock mass parameters are determined, and the Q-system is used for classification. A valley model is constructed to estimate in-situ stress and analyze stability issues with empirical, semi-analytical, and analytical methods. The paper concludes with recommendations for predicting stability issues in the higher Himalayan region.

Keywords
schistose rock, plastic zone, in-situ stresses, rock burst

1. Introduction

Nilgirikhola Hydroelectric Project is located at 35 km northeast (NE) of Beni, Maygdi, which is located in Annapurna Rural Municipality ward no 4 of Myagdi District in the Gandaki Province of Nepal. This Project is divided into two parts whereas The Nilgiri I Hydroelectric Project (40 MW) is a RoR project with the majority of its components are underground, including the Approach Tunnel, Settling Basin, Flushing Tunnel, HRT (2.25km, inverted D shape, 3m×3.5m Size), three adits, a vertical pressure shaft, and an inclined pressure shaft. Surface structures include the headworks, surge tank, and powerhouse.The project has a gross head of 482 m and an annual discharge of 15.98m^3/s. The Nilgiri II Hydroelectric Project is a Cascade type project (71 MW), with a Headrace Tunnel (4.25 km long, inverted D shape and 3×3.5m). The project has a gross head of 789.75 m and a mean annual discharge of 17.15 m^3/s. The project's components include Intake, Headrace Tunnel, four Adits, an Inclined Pressure Shaft, a Surge Tank, and a Surface Power House.This paper is focused on Nilgiri II Hydroelectric Project. During field visit it was found that following chainage were affected by Stress induced failure during construction of HRT of Nilgirikhola II Hydroelectric Project.

Table 1: Stressed induced problems encountered at different Chainages

| S.N	Chainage	Remarks
1	0+609.2 m to 0+628.2 m	Rock Bursting Occur
2	0+664.2 m to 0+672.0 m	Rock Bursting Occur
3	0+682.0 m to 0+686.2 m	Rock Bursting Occur
4	0+706.0 m to 0+712.2 m	Rock Bursting Occur
5	0+808.4 m to 0+839.45 m	Rock Bursting Occur
6	0+903.4 m to 1+045.6 m	Rock Bursting Occur
7	1+066.6 m to 1+105.2 m	Rock Bursting Occur
8	2+162 m-2+188 m	Rock Squeezing Occur
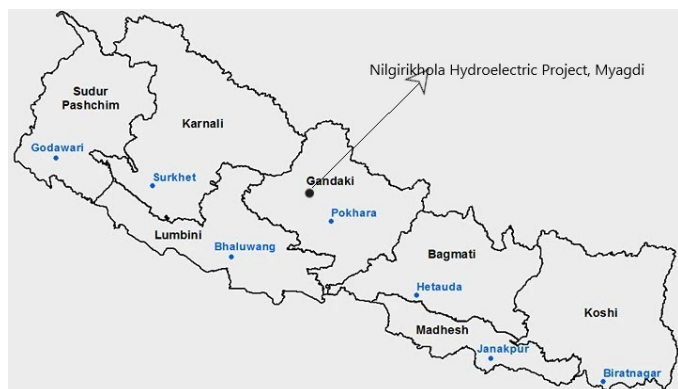
Figure 1: Location of Study Area

2. Project Geology

The study area is in the Higher Himalayan Zone, located between the South Tibetan Detachment System to the North and the Main Central Thrust to the South.It features Higher Himalayan metamorphic rocks, exposed in the Kali Gandaki gorge. The Tibetan slab is thrust over the Lesser Himalayan sequence along the Main Central Thrust. The Higher Himalayan crystallines are divided into three formations. Formation I, located north of Dana, consists of mylonitic quartzites alternating with micaceous gneisses. Formation II starts with calcareous gneisses and extends for about 2,000

meters, containing various minerals, including calcite, quartz, hornblende, and more. The Nilgiri Khola Hydroelectric Project is situated in this formation. Formation III begins with augen gneiss and features minor migmatite zones upstream of Ghasa, with the presence of ruby crystals and andalusite grains in pegmatites in the augen gneiss.
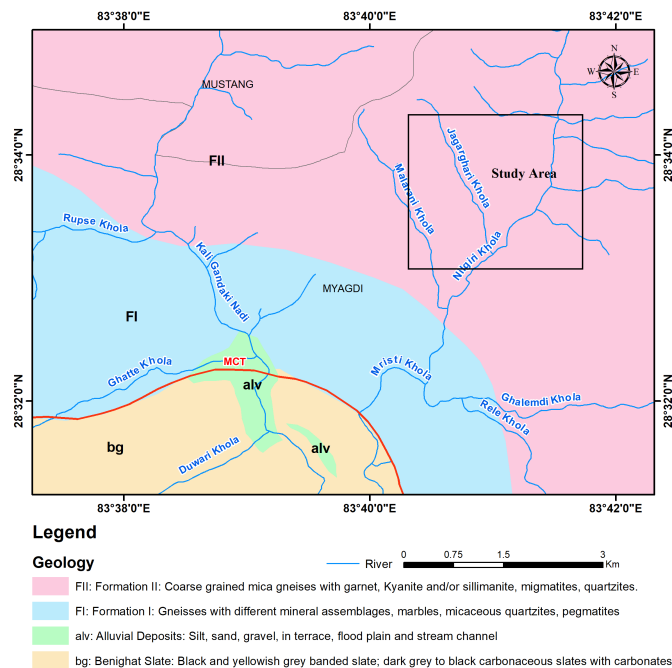
**Figure 2:** Geological Map of study area and sorroundings (Source: Department of mines and geology)
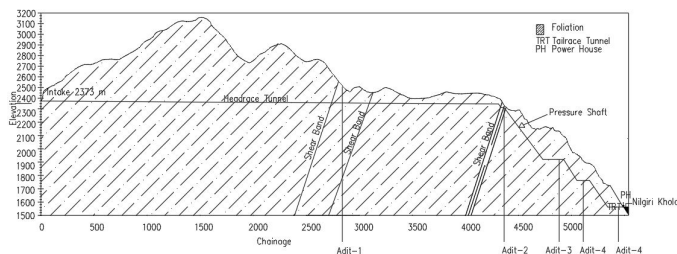
Figure 3: Longitudinal Profile of HRT

2.1 Mapped Rock Mass Quality

The rock mass classification in the headrace tunnel (HRT) employed Barton et al.'s 1974 Q-system. This assessment spanned the entire 4.2-kilometer tunnel during excavation, categorizing rock masses by Q-values. Rock masses with Q-values exceeding 40 (Q >40) are deemed to be of very good quality. Those falling within the Q-value range of 10 to 40 (40 >Q >10) are considered good rock masses. Rock masses with Q-values between 4 and 10 (10 >Q >4) are categorized as fair. Q-values ranging from 1 to 4 (4 >Q >1) indicate poor rock masses, while Q-values between 0.1 and 1 (1 >Q >0.1) signify very poor rock masses. Extremely poor rock masses are those with Q-values ranging from 0.01 to 0.1 (0.1 >Q >0.01), and exceptionally poor rock masses fall within the range of 0.01 to 0.001 (0.01 >Q >0.001). Results showed that the majority (36%) fell into the fair rock mass category, followed by very poor rock mass at 29%, and poor rock mass at 21 %. A smaller segment

(6 %) combined good and extremely poor rock masses, while exceptionally poor rock mass accounted for just 2 %. For a visual representation, refer to the accompanying Figure, illustrating rock mass distribution along the headrace tunnel alignment. Foliation is dipping toward N10°.
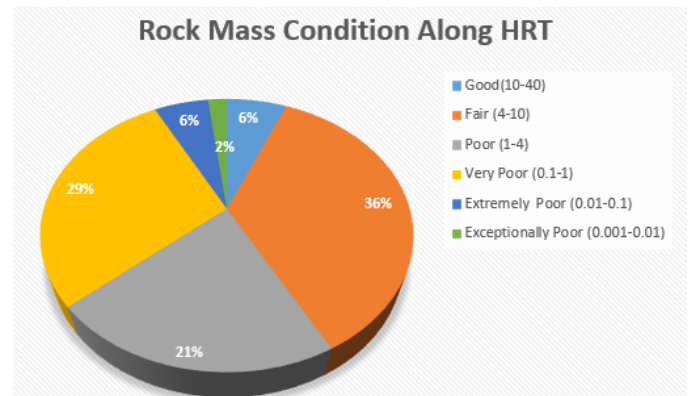
Figure 4: Actual Rock Mass Quality

3. Methodology

Review the existing body of literature, including research papers and technical reports, pertaining to the construction of hydroelectric projects in mountainous regions. Simultaneously, perform fieldwork involving site visits, surface mapping, face mapping, and interviews with project personnel, while also documenting construction activities. This comprehensive data-gathering process serves the purpose of pinpointing specific challenges encountered during project construction. Following the data collection phase, conduct an analysis to discern the contributing factors to the instability issues observed in the construction process. Utilize the gathered information to estimate rock mass properties, rock mass deformation characteristics, and in-situ stress conditions. Subsequently, proceed with a stability assessment employing a variety of empirical, semi-analytical, and analytical methods to arrive at a comprehensive evaluation of the situation.
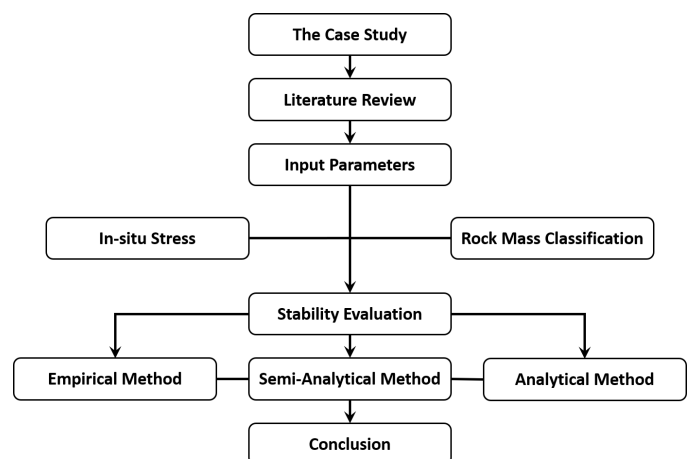
Figure 5: Methodology Step Followed During Study

4. Stability Assessment

4.1 Tunnel Alignment

Tunnel alignment selection is a critical aspect of tunneling projects, as it directly affects the safety, efficiency, and cost of construction.Joint rosette is a method commonly used to determine the optimal alignment for a tunnel. The black line in joint rosette indicates the actual tunnel alignment. The angle of tunnel from inlet portal to outlet portal is 42 ° NE and also near the predomintent joints sets. Due to this such stress induced problem like rock bursting and rock squeezing, water ingress and overbreak were occurred during construction of tunnel.So special consideration is required for safe construction activites.
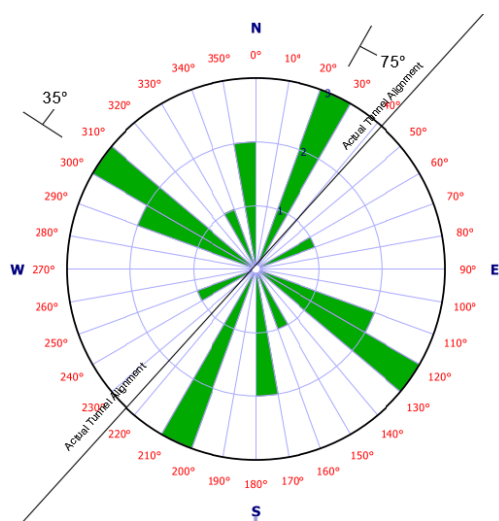

Figure 6: Joint Rosette Diagram with Actual Tunnel Alignment

4.2 Construction of Valley Model

In order to conduct an assessment of the enclosed model, it is crucial to acquire the in-situ primary stress values. To ascertain these primary stress values, a two-dimensional valley model based on the topography has been created for a specific section of the headrace tunnel during Phase 2

Table 2: Summary of input parameter

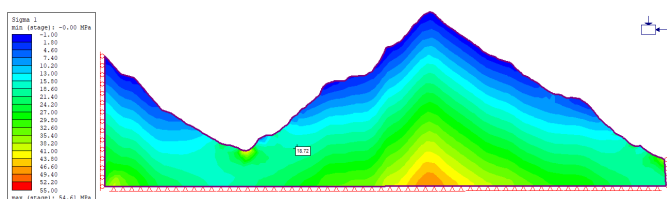| Descriptions	Unit	Value	Remarks
UCS	Mpa	79.8	Phukot Karnali PRoR HEP
E_{50}	Gpa	38.4	Phukot Karnali PRoR HEP
V_{50}		0.24	Phukot Karnali PRoR HEPt
Tectonic Stress(σ_t)	Mpa	15	Basnet and Panthi (2021)

Figure 7: Valley model construction for headrace tunnel alignment at chainage 0+615 m

Table 3: Input Parameter for Valley Model

Description		Unit	Ch 609.2-628.2 m
Over Burden	h	m	397
Poisson's Ratio	ν		0.24
Density Of Rock	γ	KN/m3	27
Tectonic stress	σ_ν	Mpa	15
Trend of Tectonic stress	θ_t	degree	N10°E
HRT trend	θ_c	degree	N42°E
Angle b/w σ_h and HRT trend	θ	degree	48
Vertical Stress	σ_ν	Mpa	10.72
Horizontal stress	σ_h	Mpa	3.38
Total Horizontal stress	σ_H	Mpa	18.38
In-plane Horizontal Stress	σ_a	Mpa	14.17
Out of plane Horizontal Stress	σ'_a	Mpa	7.60
Locked in			
In-Plane		Mpa	10.78
Out of Plane		Mpa	4.22
Stress Ratio			
In-Plane	K_H	Mpa	1.32
Out of Plane	K_h	Mpa	0.71

Table 4: Output Parameter from Valley Model

Chainage (m)	σ_1 (MPa)	σ_3 (MPa)	σ_Z (MPa)	Θ°
0+609.2-0+628.2	18.72	8.58	8.18	37
0+664.2-0+672.0	17.47	8.08	7.76	37
0+682.0-0+686.2	17.47	8.08	7.76	37
0+706-0+712.2	18.03	7.73	7.81	42
0+808.4-0+839.45	18.6	8.69	8.18	45
0+903.4-1+045.6	21.48	10.39	9.28	51
1+066.6-1+105.2	21.53	11.59	9.76	58
2+162.0-2+188.0	17.63	9.95	8.25	54

4.3 Rock Bursting Analysis

Excessive stress in the surrounding ground can lead to failure unless proper rock support is implemented. When deformations occur suddenly, this occurrence is referred to as rock bursting (Palmström, 1995). When the compressive tangential stress along the excavation surpasses the rock's strength, it results in fracturing around the tunnel's periphery. If this fracturing happens suddenly and produces loud noises from the rock, it is termed as rock bursting (Basnet, 2013)

4.3.1 The Norwegian Rule of Thumb

According to the Norwegian guideline established by Selmer-Olsen in 1965, the risk of rock spalling or rock burst increases when the depth of rock cover above the tunnel surpasses 500 meters. Even when the tunnel follows the valley side with a slope angle exceeding 25 degrees, the severity of such failures is expected to be significant.

Table 5: Rock Bursting Analysis With Noregian Rule of Thumb

S.N	Chainage (m)	Overburden	Rock Bursting
1	0+609.2-0+628.2	397	NO
2	0+664.2-0+672.0	399	NO
3	0+682.0-0+686.2	398	NO
4	0+706-0+712.2	392	NO
5	0+808.4-0+839.45	442	NO
6	0+903.4-1+045.6	602	Yes
7	1+066.6-1+105.2	665	Yes

4.3.2 Stress Problem Classification

The stress problem Classification approach primarily relies on three input factors: the intact rock strength (σ_{ci}), the maximum principal stress (σ_1) and the maximum tangential stress ($\sigma_{\theta\text{-max}}$). To apply this technique for evaluation, it's essential to possess laboratory-tested intact rock strength data and an understanding of the in-situ stress conditions in the relevant area.

Table 6: Stress Problem Classification Table

Chainage	$\frac{\sigma_{ci}}{\sigma_1}$	Panthi 2017	$\frac{\sigma_{\theta max}}{\sigma_{ci}}$	Panthi 2017
0+609.2-0+628.2	4.26	SC4	1.13	SC6
0+664.2-0+672.0	4.57	SC4	1.05	SC6
0+682.0-0+686.2	4.57	SC4	1.05	SC6
0+706-0+712.2	4.43	SC4	1.10	SC6
0+808.4-0+839.45	4.29	SC4	1.12	SC6
0+903.4-1+045.6	3.72	SC4	1.28	SC6
1+066.6-1+105.2	3.71	SC4	1.26	SC6

where, SC4- Moderate Spalling after greter than 1 hour SC6-Heavy Rock Burst and Immidiate Strain Failure

4.3.3 Modified Martin and Christiansson method

Modified Martin and Christiansson's method by incorporating rock mass strength (σ_{cm})suggested by Panthi (2006) instead rock mass spalling strength (σ_{ss})gives even realistic calculation on the depth impact (Panthi, 2012).

$$Sd = r \times \left(0.5 \times \frac{\sigma_{\theta max}}{\sigma_{cm}} - 0.52\right) \tag{1}$$

$$\sigma_{cm} = \frac{\sigma_{ci}^{1.6}}{60} \tag{2}$$

where S_d is rock bursting depth.

Table 7: Modified Martin and Christiansson method

Chainage m	σ_{cm}	r	$\sigma_{\theta max}$	$S_d m$
0+609.2-0+628.2	18.41	1.5	47.58	1.188
0+664.2-0+672.0	18.41	1.5	44.33	1.056
0+682.0-0+686.2	18.41	1.5	44.33	1.056
0+706-0+712.2	18.41	1.5	46.36	1.139
0+808.4-0+839.45	18.41	1.5	47.11	1.169
0+903.4-1+045.6	18.41	1.5	54.05	1.452
1+066.6-1+105.2	18.41	1.5	53	1.409

In case of Nilgirikhola II Hydroelectric Project the estimated depth of impact is near the measured data except 0+903.4-1+045.6 & 1+066.6- 1+105.2.

4.3.4 Russenes (1974) Approach

Russenes proposed the rock burst activity on the basis of maximum tangential stress and point load strength. point load strength is estimated using Bieniawski(1973)
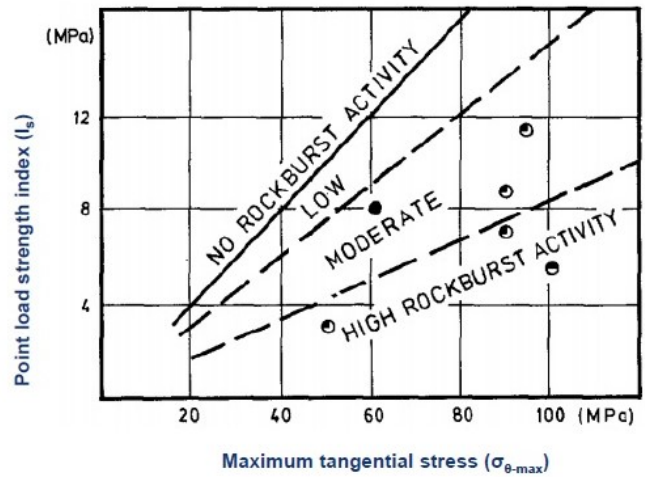
Figure 8: Russenes Chart

Table 8: Russenes Table

Chainage m	θ_{max} Mpa	I_s Mpa	Rock Burst Activity
0+609.2-0+628.2	47.58	4.988	Moderate
0+664.2-0+672.0	44.33	4.988	Moderate
0+682.0-0+686.2	44.33	4.988	Moderate
0+706-0+712.2	46.36	4.988	Moderate
0+808.4-0+839.45	47.11	4.988	Moderate
0+903.4-1+045.6	54.05	4.988	Moderate
1+066.6-1+105.2	53	4.988	Moderate

4.3.5 Hoek and Brown (1980) approach

A correlation for tangential stresses estimation is provided below based on a large number of comprehensive boundary element stress analyses (Hoek and Brown, 1980). The vertical stress computed using equation

$$\sigma_v = \gamma Z \tag{3}$$

Where γ is the specific weight of the rock mass (MN/m^3), and Z is the overburden depth in meters. The total horizontal stress is as follows:

$$\sigma_h = \frac{\sigma_v \cdot \mu}{1 - \mu} + \sigma_{tec} \tag{4}$$

Where μ is the Poisson's Ratio. Tangential stress in the roof,

$$\sigma_{\theta r} = (A_k - 1) \cdot \sigma_v \tag{5}$$

Where k is the stress anisotropy Tangential stress in the wall,

$$\sigma_\theta = (B - k) \cdot \sigma_v \tag{6}$$

A & B values for underground openings (Hoek & Brown, 1980)

4.4 Rock Squeezing Analysis

Squeezing of the rock refers to significant time-dependent deformation that occurs in the vicinity of a tunnel. This phenomenon is primarily attributed to creep resulting from the surpassing of a critical shear stress threshold (ISRM, 1995). To anticipate tunnel squeezing, various empirical approaches have been employed, including those proposed by Singh et al.

Table 9: Rock Burst Condition Table

Chainage (m)	In Roof	In Wall
0+609.2-0+628.2	Sever Spalling	Stable
0+664.2-0+672.0	Sever Spalling	Stable
0+682.0-0+686.2	Sever Spalling	Stable
0+706-0+712.2	Severe Spalling	Stable
0+808.4-0+839.45	Severe Spalling	Minor Spalling
0+903.4-1+045.6	Sever Spalling	Minor Spalling
1+066.6-1+105.2	Sever Spalling	Sever Spalling

(1992), Goel et al. (1995), the semi-analytical method introduced by Hoek and Marinos (2000), and the research conducted by Shrestha and Panthi (2015). Sections with extremely poor rock mass and exceptionally poor rock mass were taken for Squeezing study along the headrace tunnel.

4.4.1 Singh et al.(1992) Approach

A correlation for tangential stresses estimation is This method is mainly based on the rock mass classification system. Singh et al. (1992) developed an empirical relationship. Estimated Q-value is used to find the limiting overburden for tunnel.

$$H = 350 \cdot Q^{1/3} \tag{7}$$

From the above equation, it can be found that the squeezing phenomenon may occur in the rock mass when the depth of overburden above the tunnel section exceeds $350 \cdot Q^{1/3}$.

Table 10: Singh et al.(1992) Approach

Chainage m	Overburden	Q	H	Squeezing
1+487-1+503	795	0.08	150.81	Yes
1+762-1+772	546	0.002	44.10	Yes
1+772-1+802	534	0.005	59.85	Yes
2+162-2+188	538	0.008	70.00	Yes
2+372-2+382	471	0.02	95.00	Yes
2+382-2+412	461	0.008	70.00	Yes
2+412-2+422	435	0.083	152.67	Yes
2+532-2+555	409	0.083	152.67	Yes
3+993-4+063	107	0.08	150.81	No
4+113-4+203	100	0.0625	138.90	No

4.4.2 Goel et al.(1995) Approach

It is similar to Singh et. al. approach in which the limiting height depends upon Q-value without SRF. Goel et al. (1995) developed an empirical relation to calculate limiting height

$$H = 270 \cdot Q^{0.33} \cdot B^{-0.1} \tag{8}$$

Where, B = Tunnel span or height From the above equation, it can be concluded that the squeezing phenomenon may occur in the rock mass when the depth of overburden above the tunnel section exceeds $270 \cdot Q^{0.33} \cdot B^{-0.1}$.

4.4.3 Jimenez and Racio (2011) Approach

Jimenez and Racio (2011) developed an empirical relationship using 62 case study from india and Nepal. Estimated Q-value is used to find the limiting overburden for tunnel.

$$H = 424.2 \cdot Q^{0.32} \tag{9}$$

Table 11: Goel et al. (1995) Approach

Chainage m	Q (SRF=1)	Goel et al. (1995)	Squeezing
1+487-1+503	0.8	228.90	Yes
1+762-1+772	0.02	67.76	Yes
1+772-1+802	0.05	91.68	Yes
2+162-2+188	0.08	107.06	Yes
2+372-2+382	0.2	144.86	Yes
2+382-2+412	0.08	107.06	Yes
2+412-2+422	0.83	231.69	Yes
2+532-2+555	0.83	231.69	Yes
3+993-4+063	0.8	228.90	No
4+113-4+203	0.625	210.99	No

From the above equation, it can be found that the squeezing phenomenon may occur in the rock mass when the depth of overburden above the tunnel section exceeds $424.2 \cdot Q^{0.32}$.

Table 12: Jimenez and Racio (2011) Approach

Chainage m	Jimenez and Racio (2011)	Squeezing
1+487-1+503	189.04	Yes
1+762-1+772	58.06	Yes
1+772-1+802	77.85	Yes
2+162-2+188	90.48	Yes
2+372-2+382	121.31	Yes
2+382-2+412	90.48	Yes
2+412-2+422	191.28	Yes
2+532-2+555	191.28	Yes
3+993-4+063	189.04	No
4+113-4+203	174.68	No

4.4.4 Hoek and Marinos(2000) Approach

Hoek and Marinos (2000) proposed following equations to determine size of the plastic zone and deformation of a tunnel in weak rock mass condition.

$$\frac{\delta_i}{d_o} = \left(0.002 - 0.0025\frac{p_i}{p_o}\right)\left(\frac{\sigma_{cm}}{p_o}\right)^{2.4\frac{p_i}{p_o}-2} \tag{10}$$

$$\frac{\delta_i}{d_o} = \left(1.25 - 0.625\frac{p_i}{p_o}\right)\left(\frac{\sigma_{cm}}{p_o}\right)^{p_i/p_o-0.57} \tag{11}$$

Where, d_p = Plastic zone diameter, d_o = Original tunnel diameter in meters, δ_i = Tunnel sidewall deformation, p_i = Internal support pressure, p_o = In situ stress = depth × unit weight, and σ_{cm} = Rock mass strength.
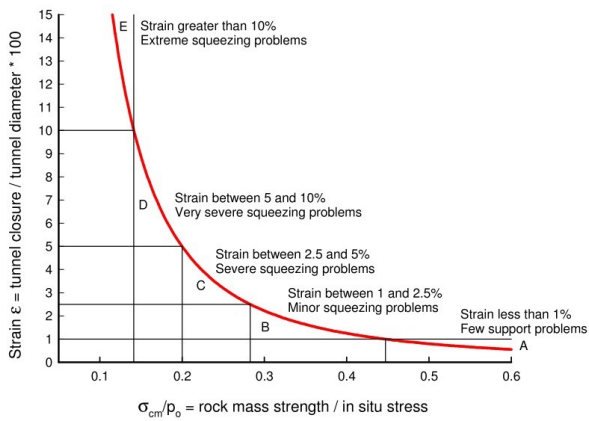
Figure 9: Classification of squeezing behavior (Hoek & Marinos, 2000)

Table 13: Hoek & Marinos, 2000 Approach

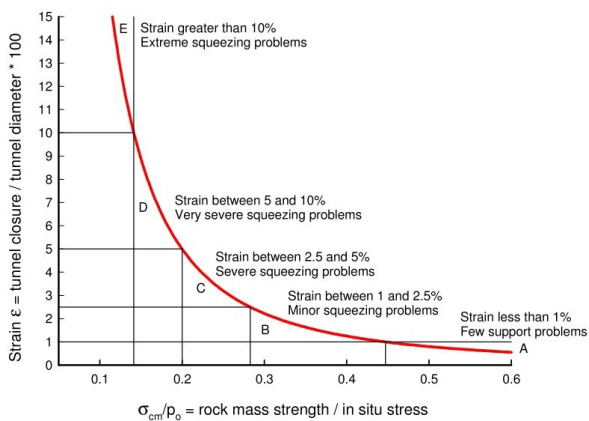| Chainage (m)	Rockmass	ϵ (Pi=0)	δ_i (mm)
1+487-1+503	BG	0.0182	56.39
1+762-1+772	BG	0.0086	26.60
1+772-1+802	BG	0.0082	25.44
2+188-2+162	BG	0.0083	25.82
2+372-2+382	BG	0.0064	19.79
2+382-2+412	BG	0.0061	18.96
2+412-2+422	BG	0.0054	16.88
2+532-2+555	BG	0.0048	14.92
3+993-4+063	BG	0.0003	1.02

Figure 10: Enter Caption

4.4.5 Shrestha and Panthi (2018) Approach

A research paper on estimating tunnel strain in the weak and schistose rock mass influenced by stress anisotropy: an evaluation based on three tunnel cases from Nepal (Shrestha & Panthi, 2018) recommends the following equation to find instantaneous and final closure of tunnel. This equation uses rock mass shear modulus (G), vertical stress (σ_v), support pressure (P_i), and stress ratio (k).

$$\epsilon_{ic} = 3065 \left(\frac{2G(1 + p_i)}{\frac{\sigma_v(1+k)}{2}} \right)^{-2.13} \tag{12}$$

$$\epsilon_{fc} = 4509 \left(\frac{2G(1 + p_i)}{\frac{\sigma_v(1+k)}{2}} \right)^{-2.09} \tag{13}$$

Where, ϵ_{ic} = Instantaneous closure, ϵ_{fc} = Final closure.

Table 14: Shrestha & Panthi, 2018 Approach

Chainage (m)	ϵ_{ic}	δ_I (m)	ϵ_{fc}	δ_F (m)
1+487-1+503	0.105	0.325	0.187	0.580
1+762-1+772	0.047	0.146	0.085	0.264
1+772-1+802	0.045	0.139	0.081	0.252
2+188-2+162	0.046	0.141	0.083	0.256
2+372-2+382	0.034	0.107	0.063	0.194
2+382-2+412	0.033	0.102	0.060	0.186
2+412-2+422	0.029	0.090	0.053	0.164
2+532-2+555	0.025	0.079	0.047	0.145
3+993-4+063	0.001	0.005	0.003	0.009
4+113-4+203	0.001	0.004	0.002	0.008

4.4.6 Analytical method (Rock support interaction)

The Convergence Confinement Method (CCM) is used to establish the interrelationship between the Ground Reaction Curve (GRC), Longitudinal Deformation Profile (LDP), and Support Characteristics Curve (SCC). These methods are pivotal for optimizing support systems. The displacements calculated through the CCM are utilized to validate the numerical modeling results.. First, we have to calculate hydrostatic stresses P_o and uniform internal support pressure P_i. These pressures are subjected to the support applied in the section. The supports generally used are shotcrete, systematic bolting, and steel ribs. If the internal support pressure P_i is greater than the pressure at which maximum deformation takes place P_{sD}, then no failure will occur, which helps to optimize the supports.The Support Characteristics Curve is formulated through the utilization of shotcrete or concrete and steel ribs. The shotcrete or concrete linings are characterized by specific parameters, including an unconfined compressive strength of 35 MPa, a thickness of 150 mm (adjusted according to the rock class), a Poisson's ratio of 0.2, and a Young's modulus of elasticity of 25 GPa. The maximum pressure exerted by the shotcrete lining is determined based on the findings of Carranza-Torres and Fairhurst (2000), while block steel sets of ISMB 150 are placed at 1-meter intervals in the field.

Table 15: Input parameter for CCM

Parameter	For Ch 2+162 m
Radius of Tunnel R (m)	1.55
Unit Weight of Rock γ [MN/m³]	0.027
Loading σ_0 [MPa]	15.704
UCS σ_{ci} [MPa]	79.8
Hoek and Brown Parameter mi	28
Poisson's Ratio ν	0.24
Dilation angle ψ [deg]	0
GSI	20
Face effect L (m)	1
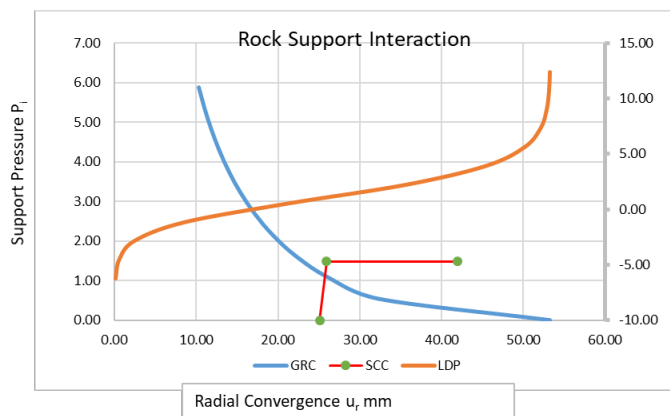
Figure 11: Rock Support Interaction For Ch 2+162

Table 16: Output parameter from CCM

Parameter	For Ch 2+162 m
Po (MPa)	14.52
Picr (MPa)	5.95
u_{rmax} (u_r) mm when P_i=0	53.97 mm
u_r at face (mm)	18 mm
u_r at 1m (mm)	25.45 mm
Psmax (MPa)	1.49

5. Conclusion

Following are the major conclusion from this study

- The highest percentage with 36 % of overall Rock mass classification consists of fair Rock mass, 29% consists of very poor rock mass, 21% consists of Poor Rock mass, 6% consist of both Good and Extremely poor rock mass and 2% consist of exceptionally poor rock mass observed in Headrace Tunnel of Nilgirikhola Hydroelectric Project.

- According to the joint rosette diagram, it indicates stability issues caused by the tunnel's alignment being near predominant joint sets and the tunnel alignment direction opposing the dip. Therefore, special considerations are required for safe construction activities.

- The empirical approaches by Singh et al (1992), Goel et al (1995) and Jimenez and Recio (2011) shows that squeezing occurs at Ch 1+487-1+503, Ch 1+762-1+772, Ch 1+772-1+802, Ch 2+162 - 2+188, Ch 2+372-2+382, Ch 2+382-2+412, Ch 2+412-2+422 and Ch 2+532-2+555.

- According to the CCM method, it shows that the support installed as adopted by the project is just adequate and possibility of further squeezing.

- At chainage 2+162 to 2+188, according to the method by Hoek and Marinos (2000), only 25.82 mm of deformation obtain with no support pressure. This appears to be conservative. According to the approach by Shrestha and Panthi (2000), the final inward deformation is 25.6 cm with no support pressure, while the measured final inward deformation in the field is 16 cm.

- Rock Bursting analysis was done it shows that Hoek and Brown 1980, Russens (1974) Approach and Stress Problem Classification using panthi (2017) are effective for the prediction of rock bursting/spalling and Modified Martin and Christiansson's method is effective for determination of rock bursting depth.

Acknowledgments

References

[1] Barton, et al. (1974). Using the Q-system: rock mass classification and support design. Norwegian Geotechnical Institute, 57.

[2] Dhital, M. R. (2015). Geology of the Nepal Himalaya Regional Perspective of the Classic Collided Orogen.

[3] Basnet, C. B. (2013). Evaluation on the Squeezing Phenomenon at the Headrace Tunnel of Chameliya Hydroelectric Project, Nepal. June.

[4] Bieniawski, Z. T. (2014). Short on the RMR (Rock Mass Rating) system. Www.Rockmass.Net, 1–3.

[5] Hoek, E., & Marinos, P. (2000). Predicting tunnel squeezing problem in weak heterogeneous rock masses. Tunnels and Tunnelling International, 45–51.

[6] Palmström, A. (1995). Characterizing Rock Burst and Squeezing by the Rock Mass Index. Design and Construction of Underground Structures, c(February), 23–25.

[7] Panthi, K. (2006). Analysis of Engineering Geological Uncertainties Related to Tunnelling in Himalayan Rock Mass Conditions. In Norwegian University of Science and Technology (Vol. 5, Issue February).

[8] Shrestha, P. K., & Panthi, K. K. (2018). Estimating Tunnel Strain in the Weak and Schistose Rock Mass Influenced by Stress Anisotropy: An Evaluation Based on Three Tunnel Cases from Nepal. Rock Mechanics and Rock Engineering, 51(6), 1823–1838. https://doi.org/10.1007/s00603-018-1448-7

[9] Zare, S. (2007). Drill and Blast Tunnelling Blast Design.

[10] Panthi, K., & Nilsen, B. (2005). Significance of grouting for controlling leakage in water tunnels: A case from Nepal. Proceedings of ITA-AITES 2005 world tunnelling congress and 31st ITA General Assembly, Istanbul, Turkey, 2005. 931-937.

[11] Panthi, K. K. (2011). Assessment on stress-induced instability in a tunnel project of the Himalaya. 12th ISRM Congress, 2011. OnePetro.

[12] Shrestha, G. L., & Broch, E. (2008). Influences of the valley morphology and rock mass strength on tunnel convergence: with a case study of Khimti 1 headrace tunnel in Nepal. Tunnelling and Underground Space Technology, 23, 638-650.

[13] Shrestha, P. K., & Panthi, K. K. (2014). Analysis of the plastic deformation behavior of schist and schistose mica

gneiss at Khimti headrace tunnel, Nepal. Bulletin of Engineering Geology and the Environment, 73, 759-773.

[14] Shrestha, P. K., & Panthi, K. K. (2015). Assessment of the effect of stress anisotropy on tunnel deformation in the Kaligandaki project in Nepal.

[15] Jimenez, R. & Recio, D. (2011) A linear classifier for probabilistic prediction of squeezing conditions in Himalayan tunnels.

[16] Farhadian, H. and Nikvar-Hassani, A. (2020) Development of a new empirical method for Tunnel Squeezing Classification (TSC).

[17] Basnet, C. B. & Panthi, K. K. (2018) Evaluation of in-situ stress state along the shotcrete lined high-pressure headrace tunnel at a complex Himalayan geological condition.

[18] Chhatra Bahadur Basnet & Krishna Kanta Panthi (2021) Evaluation of in-situ stress state along the shotcrete lined high-pressure headrace tunnel at a complex Himalayan geological condition, Geosystem Engineering, 24:1, 1-17